ISSN 1063-7834, Physics of the Solid State, 2013, Vol. 55, No. 11, pp. 2191–2195. © Pleiades Publishing, Ltd., 2013.
Original Russian Text © Yu.V. Knyazev, A.V. Lukoyanov, Yu.I. Kuz'min, A.G. Kuchin, 2013, published in Fizika Tverdogo Tela, 2013, Vol. 55, No. 11, pp. 2081–2085.

METALS

Specific Features of the Electronic Structure and Spectral Properties of $NdNi_{5-x}Cu_x$ Compounds

Yu. V. Knyazev[a, *], A. V. Lukoyanov[a, b], Yu. I. Kuz'min[a], and A. G. Kuchin[a]

[a] *Institute of Metal Physics, Ural Branch of the Russian Academy of Sciences, ul. Sofii Kovalevskoj 18, Yekaterinburg, 620990 Russia*

* *e-mail: knyazev@imp.uran.ru*

[b] *Ural Federal University named after the First President of Russia B. N. Yeltsin (Ural State Technical University–UPI), ul. Mira 19, Yekaterinburg, 620002 Russia*

Received April 10, 2013

Abstract—The spectral properties of the intermetallic compounds $NdNi_{5-x}Cu_x$ ($x = 0, 1, 2$) have been studied using optical ellipsometry in the wavelength range 0.22–16 μm. It has been established that substitution of copper atoms for nickel leads to noticeable changes in the optical absorption spectra, plasma frequencies, and relaxation frequencies of conduction electrons. Spin-polarized calculations of the electronic structure of these compounds have been performed in the local spin density approximation allowing for strong electron correlations (LSDA + U method) in the 4f shell of the rare-earth ion. The calculated electron densities of states have been used to interpret the experimental dispersion curves of optical conductivity in the interband light absorption region.

DOI: 10.1134/S1063783413110115

1. INTRODUCTION

Intermetallic compounds of rare-earth elements R with nickel of the type RNi_5 stand out in the large variety of their magnetic structures and electronic characteristics. The unique features of the physicochemical properties of these alloys underlie their engineering potential as functional materials for permanent magnets and magnetothermal applications, as well as for devices based on magnetostriction and magnetoresistive effects [1–3]. Particular interest expressed in investigation of the properties of RNi_5 compounds stems from their ability to absorb and accumulate atomic hydrogen [4], which led to the development of portable energy-intensive storage cells based on (Ni–R–H) [5].

The specific features in the magnetic and electronic properties of the RNi_5 intermetallic compounds are associated with the Ni 3d bands being practically fully occupied by 5d electrons of the outer shells of R atoms, which makes the contribution of Ni atoms to the spontaneous magnetic moment weak. Magnetic ordering in alloys of this system is mediated by indirect exchange interaction among R ions supported by conduction electrons, as well as by crystal field effects. It was found that many of the physical properties of the RNi_5 compounds change significantly when Ni is substituted for by atoms of other d or p metals as a result of the strong effect an impurity exerts on the parameters of the electronic structure, crystal field, and exchange interaction. For instance, various pseudobinary $RNi_{5-x}M_x$ alloys (M = Al, Cu, Fe, Co), which are solid solutions with the structure of the parent binary compound, exhibit nonmonotonic concentration dependences of the crystalline, electronic, magnetic, and thermodynamic characteristics [6–9]. Doping likewise brings about a substantial improvement of the electrochemical characteristics affecting the ability of these materials to absorb atomic hydrogen [4, 10].

Substantial modifications of the above properties imparted by an increase of the concentration of Cu impurity were found also in the $NdNi_{5-x}Cu_x$ ($x \le 2$) system of ferromagnetic intermetallic compounds with low magnetic transition points (the Curie temperature T_C for $NdNi_5$ is close to 8 K) [7]. Growth of the number of substituent atoms leads to a decrease of the spontaneous magnetic moment and magnetic susceptibility, nonmonotonic variation of T_C, as well as structural and electronic characteristics [7, 11]. X-ray photoemission measurements [11, 12] demonstrate noticeable transformation of the energy bands of these alloys below the Fermi level E_F, which is induced by a partial substitution of copper atoms for nickel. This was found to be accompanied by the appearance in the valence-band photoemission spectrum of a broad maximum at the binding energy ~3.5 eV, which was identified with the Cu 3d band. Its intensity depends directly on the impurity concentration, with the main contribution to the electron densities of states in the range of up to 6 eV below E_F being provided by the narrow Nd 4f and wide Ni 3d bands.

Additional information on the specific features in the effect of an impurity on band structure evolution of

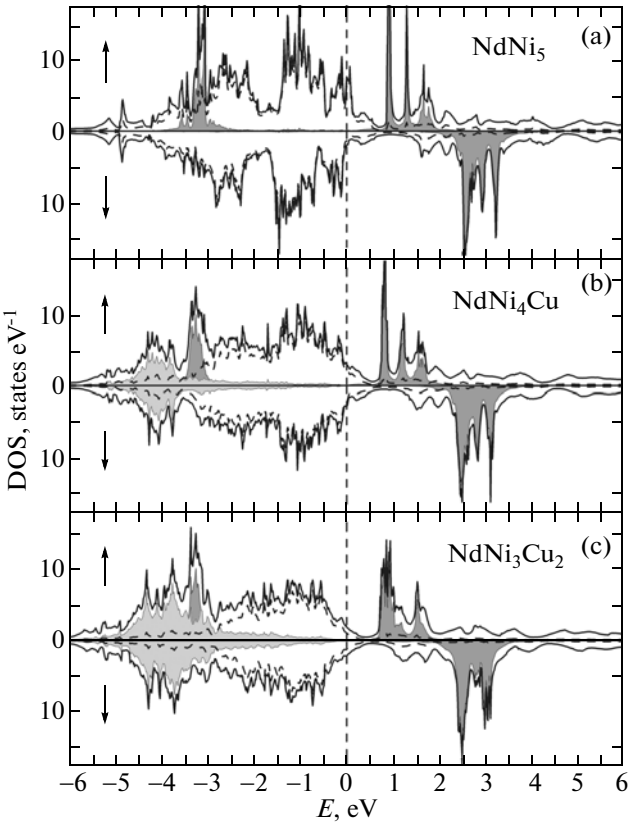

Fig. 1. Total (solid curve) and partial for Ni 3*d* (dashed curves), Nd 4*f* (dark-gray regions), and Cu 3*d* (light-gray regions) densities of states calculated for (a) $NdNi_5$, (b) $NdNi_4Cu$, and (c) $NdNi_3Cu_2$ compounds in the framework of the LSDA + *U* method. The Fermi level corresponds to zero on the energy scale.

these compounds can be obtained from integrated studies of spectral characteristics and band calculations of energy spectra. In this work, the electronic properties of alloys in the $NdNi_{5-x}Cu_x$ ($x = 0, 1, 2$) system have been investigated using the LSDA + *U* calculations of the energy band spectrum and measurements of the frequency dependences of optical parameters. The main structural features of the dispersion curves of interband optical conductivity have been interpreted based on the calculated electron densities of states. The experimental data complemented by the calculations provide information on the principal characteristics of the band spectrum and their variation with increasing number of substituent atoms.

2. CALCULATION OF THE ELECTRON DENSITY OF STATES

The $NdNi_{5-x}Cu_x$ ($x = 0, 1, 2$) alloys have a $CaCu_5$-type hexagonal structure with *P*6/*mmm* space symmetry group. Nd atoms in the $NdNi_5$ unit cell consisting of one formula unit occupy the 1*a* (0, 0, 0) crystallographic position, while Ni atoms are localized in two symmetrically inequivalent positions 2*c* (1/3, 2/3, 0) and 3*g* (1/2, 0, 1/2). The *a* and *c* parameters of the hexagonal lattice increase with increasing Cu content to become $a = 4.956$ Å, $c = 3.950$ Å for $NdNi_5$, $a = 4.984$ Å, $c = 3.991$ Å for $NdNi_4Cu$, and $a = 5.006$ Å, $c = 4.014$ Å for $NdNi_3Cu_2$. The self-consistent calculations of the electronic structure of these compounds were performed in the local electronic density approximation allowing for the strong interactions of 4*f* electrons of Nd atoms (the LSDA + *U* method [13]). The parameters of the direct Coulomb and exchange interactions for the Nd 4*f* shell were calculated in the present study in the frame of the supercell procedure and found to be $U = 4.2$ eV and $J = 0.7$ eV, in contrast to the values of $U = 6.25$ eV and $J = 0.9$ eV used earlier [11] as fitting parameters. The calculations were performed with the TB-LMTO-ASA code [14] with the method of linearized muffin-tin orbitals in the atomic sphere approximation. The integration by the tetrahedron method was performed on a *k*-point grid in reciprocal space with a total number $10 \times 10 \times 10 = 1000$ (186 irreducible *k*-points). The orbital basis included MT orbitals corresponding to the 6*s*, 6*p*, 5*d*, and 4*f* Nd states, as well as to the 4*s*, 4*p*, and 3*d* Ni states. The MT sphere radii of Nd were 3.6 and 2.7 a.u. for Ni in positions of both types. The calculations modeled collinear ferromagnetic ordering of local magnetic moments on all lattice sites, with spin-orbit interaction disregarded in the calculations. The values of the magnetic moment on Nd ions are close to 3.1 μ_B in all compounds, less than 0.2 μ_B on Ni ions in $NdNi_5$, and less than 0.02 μ_B in copper alloys. The calculations performed for alloys with copper were complemented for each value $x = 1$ and 2 with separate calculations for each of possible configurations of substitution of copper atoms for nickel in the unit cell, followed by averaging of the self-consistent electron densities of states with the corresponding weights.

Figure 1 presents the total electron densities of states $N(E)$ of $NdNi_{5-x}Cu_x$ compounds ($x = 0, 1, 2$) calculated for two opposite spin directions, ↑ and ↓. Also the partial density distribution for Nd 4*f* electrons, as well as for the 3*d* electrons of Ni and Cu, is shown. In all the three compounds, the extended many-peak $N(E)$ structure related with the Ni 3*d* band is nearly identical in shape for both spin orientations. The region of higher densities of states formed by electrons of a given type is localized in the occupied part of the valence band at energies 0–5 eV below E_F. The strong peaks in the ↑ band system located within 3.0–3.5 eV below and 0.7–1.8 eV above the Fermi level originate from the $4f_\uparrow$ electrons of Nd atoms. As strong peaks in the $4f_\downarrow$ band system are confined in the range 2.2–3.4 eV. Significantly, the 4*f* band structure obtained in this calculation for the two spin orientations differs from the one observed in the densities of state of structurally similar $RNi_{5-x}Cu_x$ compounds [15, 16], where *R* stands for Tb, Ho, and Er are the elements of the subgroup of heavy REM. In the latter

case, the occupied $4f_\uparrow$ and $4f_\downarrow$ bands lie deep relative to E_F (at −8 and −6 eV, respectively), and the system of very narrow (~0.1 eV) unoccupied $4f_\downarrow$ bands is localized in the range 1–2 eV above E_F.

Thus, as the content of Cu atoms increases ($x = 1$, 2), the structure of the energy dependence $N(E)$ is seen to vary primarily at energies below E_F. As shown by the calculations, substitution of copper atoms for nickel leads to a noticeable redistribution of the density of states in the range ~(3–5) eV below the Fermi level, with the minimum observed in the corresponding graph of the binary alloy at ~2 eV disappearing. The transformation of $N(E)$ is paralleled by formation of a new structure made up by a group of maxima genetically related to the Cu 3*d* band. As follows from Figs. 1b and 1c), the intensity and width of this structure depend noticeably on the copper atom concentration. Significantly, the energy of Cu 3*d* band localization obtained in the calculation is close in magnitude to the one found earlier for other compounds of this type [15, 16]. Meanwhile, the study of the band structure of isostructural intermetallic compounds of the $TbNi_{5-x}Al_x$ system [17] established that the wave function of Al 3*p* electrons in the valence band is more delocalized, with the corresponding contribution to the density of states acquiring a nearly structureless shape and being distributed uniformly over a broad energy region.

The energy dependences of the electron densities of states presented graphically in Fig. 1 correlate nicely with the experimental photoemission spectra of these compounds [11, 12]. The position, width, and intensity of the main structural features of these spectra related to the 3*d* bands of Ni and Cu atoms lying below the Fermi level are similar to those calculated in the present work.

3. RESULTS AND DISCUSSION

The technique employed in obtaining the compounds under study and their characterization are described in [7]. The spectral properties of the samples were studied in the wavelength range $\lambda = 0.22$–16 μm (0.078–5.64 eV). The optical constants, such as the refractive, $n(\lambda)$, and absorption, $k(\lambda)$, indices were measured by the ellipsometric method under single- and double reflection of light with an error of 2–4%. The mirror finish surfaces of grade 14 were prepared by mechanical polishing with fine diamond pastes. The values of n and k thus obtained can now be used to calculate the dielectric functions defining the optical response of the medium, including the most sensitive spectral parameter, namely, the optical conductivity $\sigma(\omega) = nk\omega/2\pi$ (ω is the light-wave cyclic frequency) discussed in the present paper.

Figure 2 plots dispersion curves of the optical conductivity of alloys in the $NdNi_{5-x}Cu_x$ system ($x = 0$, 1, 2). The behavior of $\sigma(\omega)$ for all compounds, irrespective of x, on the whole, is typical of the media with metallic conduction, which is demonstrated by a sharp low-energy drop at $E < 0.5$ eV that is of the Drude mechanism of electromagnetic wave absorption ($\sigma \sim \omega^{-2}$). As the light frequency increases, the pattern of dispersion of the optical conductivity of all alloys evidences the dominant part played by interband absorption, whose low-energy threshold lies below 1 eV. We see that the width of the quantum absorption band remains nearly constant for all values of x, while its structure transforms noticeably with variation of the impurity content. Indeed, the strong maximum in the $\sigma(\omega)$ spectrum of binary $NdNi_5$ located at 1.15 eV (the upper curve) becomes less pronounced in the $x = 1$ alloy, to practically disappear in the curve for the $x = 2$ compound. The broad maximum at 3.3 eV, in its turn, is conspicuous only in the $\sigma(\omega)$ graph of the ternary compound $NdNi_4Cu$, to be only weakly evident in the corresponding dispersion curves plotted for the other two alloys.

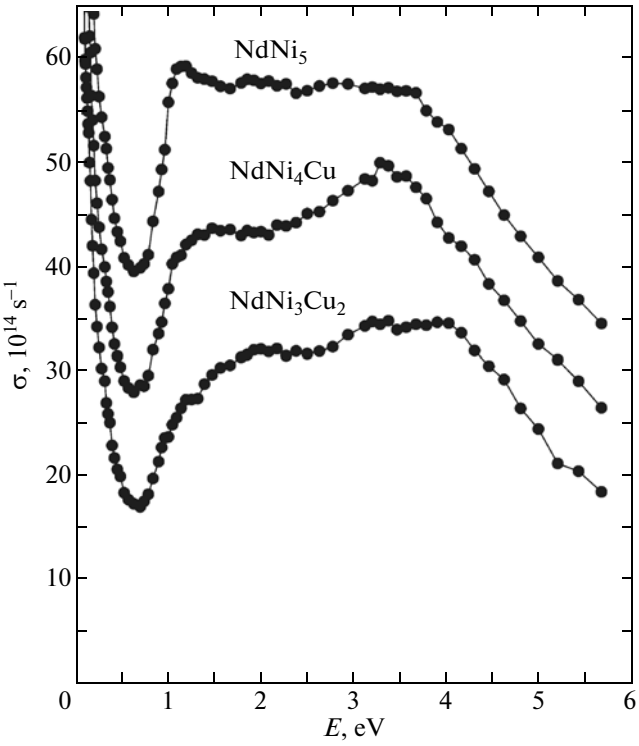

Fig. 2. Energy dependences of the optical conductivity of $NdNi_{5-x}Cu_x$ compounds ($x = 0$, 1, 2). The curves are shifted upward along the ordinate axis relative to one another by 10 units.

The specific pattern of the $\sigma(\omega)$ curves in the quantum absorption region, as well as their modification induced by substitution of copper atoms for nickel, are defined by the actual structure of energy spectra. It appears therefore of interest to compare the experimental interband optical conductivities $\sigma_{ib}(\omega)$ with the conductivities calculated from the corresponding

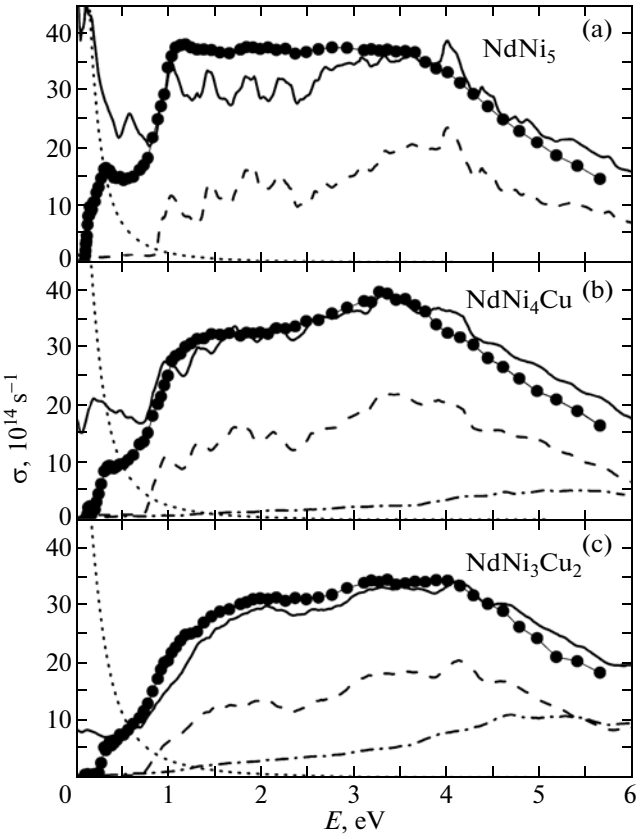

Fig. 3. Interband optical conductivity spectra of $NdNi_5$, $NdNi_4Cu$, and $NdNi_3Cu_2$. Circles refer to experiment, and the solid curve corresponds to calculation in arbitrary units. Dashed and dash-dotted curves visualize partial contributions of quantum transitions involving Nd 4*f* and Cu 3*d* electrons, respectively. Dotted line identifies the Drude contribution.

electron densities of states. These dispersion curves were obtained by subtracting the Drude contributions from experimental spectra. The theoretical interband optical conductivities were obtained, in their turn, by the method described in [18] and can be represented as an integral function obtained by convolution of the total densities of states above and below E_F. This calculation performed in arbitrary units assuming equal probabilities of direct and indirect transitions is displayed in Fig. 3 together with experimental $\sigma_{ib}(\omega)$ curves. Also shown are partial contributions to interband optical conductivity from quantum transitions involving electrons of the Cu 3*d* and Nd 4*f* bands.

A comparison shows that, for all the three alloys, the dispersion of the theoretical curves $\sigma_{ib}(\omega)$ qualitatively reproduces the main features of experimental spectra and such parameters as the range of strong absorption, its low-energy threshold, and the smooth decrease at energies above 4 eV. The pattern observed in transformation of the calculated interband optical conductivity spectra with increasing number of substituent atoms fits, on the whole, the pattern seen in experiment. For all the alloys studied, the fine structure in $\sigma_{ib}(\omega)$ spectra obtained from the total densities of states is qualitatively similar to the corresponding dispersion curves determined by the partial interband contributions involving Nd 4*f* electrons (Ni 3*d* $\longrightarrow$ Nd 4*f* transitions in the $\uparrow$ and $\downarrow$ spin subbands, as well as the Nd $4f_\uparrow \longrightarrow$ Nd $4f_\uparrow$ transitions). This suggests a significant part played by the Nd 4*f* electrons in mediating interband absorption in $NdNi_{5-x}Cu_x$ compounds. This specific feature of quantum excitation of electrons by light waves of different frequencies differs radically from the situation observed in absorption spectra of $RNi_{5-x}Cu_x$ intermetallic compounds, where *R* stands for heavy REMs. In the latter, the nature of interband absorption in the spectral region studied was found [15, 16] to evolve primarily from electron transitions between the extended Ni 3*d* bands lying below and above E_F, the contribution of the transitions involving the narrow $4f_\downarrow$ bands localized above E_F being very small. At the same time, because of the purely qualitative approach to the $\sigma_{ib}(\omega)$ calculation which disregarded the interband transition probability and the lifetime of excited state, the details of the fine structure in the experimental and theoretical behavior of interband optical conductivity are not completely identical. To cite an example, the magnitude of $\sigma_{ib}(\omega)$ calculated for a binary alloy in the low-energy range $E \leq 0.7$ eV is certainly an overestimate for a binary alloy, and a number of narrow peaks appearing in theoretical curves for alloys with $x = 0$, 1 were not confirmed by experiment.

Note that the experimental spectra visualizing the interband optical conductivity of alloys with $x = 1$ and 2 (Figs. 3b, 3c) do not reveal any conspicuous features which could be assigned to Cu 3*d* electrons, while in the density-of-states graphs (Fig. 1) the corresponding bands are denoted by strong maxima. The partial contribution of such transitions to $\sigma_{ib}(\omega)$ calculated for these compounds appears as an extended band with a broad maximum near 5 eV (Figs. 3b, 3c). It appears only natural that in the total graph depicting the interband optical conductivity this contribution is practically unseen as a result of being noticeably smeared and distributed smoothly almost over the whole energy region studied. The similar pattern of the Cu impurity band distribution in the optical spectra of the alloys under study likewise is at odds with the one observed in the isostructural intermetallic compounds of the $RNi_{5-x}Cu_x$ family (*R* stands here for heavy REM) [15, 16]. The experimental $\sigma_{ib}(\omega)$ dispersion curves obtained for these compounds demonstrate formation under substitution of copper atoms for nickel of a new strong quantum absorption band within a limited energy range of 3.5–5.0 eV, which is mediated by Cu 3*d* $\longrightarrow$ Ni 3*d* transitions in both spin subbands.

Measurement optical constants in the low-energy (Drude) spectral region where interband transitions affect only weakly optical properties offers a possibility

of calculating the relaxation, γ, and plasma, ω_p, frequencies of conduction electrons. It was established that the relaxation frequency $\gamma = 2\pi/\tau$ (τ is the relaxation time), which additively takes into account all kinds of scattering of electrons excited by an electromagnetic wave, increases substantially with increasing content of the Cu impurity and assumes the values 2.1×10^{14} s^{-1} ($NdNi_5$), 2.8×10^{14} s^{-1} ($NdNi_4Cu$) and 3.3×10^{14} s^{-1} ($NdNi_3Cu_2$). A similar trend in variation becomes evident in the magnitude of the squared plasma frequency ω_p^2, a parameter depending on interelectron correlation and structure of the electron spectrum in the near-Fermi region [19]: 26×10^{30} s^{-2} ($NdNi_5$), 31×10^{30} s^{-2} ($NdNi_4Cu$) and 35×10^{30} s^{-2} ($NdNi_3Cu_2$). The above numerical values of γ and ω_p^2 were employed in calculation of the Drude contribution to the optical conductivity, which is displayed graphically in Fig. 3.

4. CONCLUSIONS

The electronic structure and spectral properties of the isostructural compounds $NdNi_{5-x}Cu_x$ ($x = 0, 1, 2$) have been investigated. The main features in the evolution of the interband optical conductivity spectra induced by substitution of copper atoms for nickel have been identified. The spin-polarized electron densities of states have been calculated by the LSDA + U self-consistent method for all intermetallic compounds allowing for the strong correlations in the 4f shell of Nd ions. The nature of the energy bands contributing to optical absorption which evolved in the energy range under study has been established. The main structural features observed in the experimental graphs of optical conductivity were identified with the theoretical dispersion curves. It was demonstrated that the pattern of dispersion of experimental $\sigma(\omega)$ curves in the interband transition region finds a satisfactory interpretation in the frame of the $N(E)$ calculation presented. A number of differences between the interband conductivity spectra of these compounds and the corresponding dispersion curves obtained for isostructural intermetallic compounds with heavy REM were identified. The optical data obtained in the Drude frequency range were used to obtain the relaxation and plasma frequencies of conduction electrons.

ACKNOWLEDGMENTS

This study was supported by the Russian Foundation for Basic Research (project no. 13-02-00256), the Ministry of Education and Science of the Russian Federation (agreement no. 14.A18.21.0076), the Analytical Departmental Target Program "Development of the Scientific Potential of the Higher School," and the "Dynasty" Foundation.

REFERENCES

1. É. Trémolet de Lacheisserie, D. Gignoux, and M. Schlenker, *Magnetism: Materials and Applications* (Springer-Verlag, Berlin, 2005).
2. N. V. Mushnikov, Phys.—Usp. **55** (4), 421 (2012).
3. K. A. Gschneidner, Jr., V. K. Pecharsky, and A. O. Tsokol, Rep. Prog. Phys. **68**, 1479 (2005).
4. B. Sakintuna, F. Lamari-Darkrim, and M. Hirscher, Int. J. Hydrogen Energy **32**, 1121 (2007).
5. X. Zhao and L. Ma, Int. J. Hydrogen Energy **34**, 4788 (2009).
6. E. Burzo, A. Takàcs, M. Neumann, and L. Chioncel, Phys. Status Solidi. C **1**, 3343 (2004).
7. A. G. Kuchin, A. S. Ermolenko, Yu. A. Kulikov, V. I. Khrabrov, E. V. Rosenfeld, G. M. Makarova, T. P. Lapina, and Ye. V. Belozerov, J. Magn. Magn. Mater. **303**, 119 (2006).
8. A. V. Lukoyanov, A. Haldar, A. Das, A. K. Nayak, K. G. Suresh, and A. K. Nigam, J. Appl. Phys. **109**, 07E152 (2011).
9. A. Bajorek, G. Chelkowska, and B. Andrzejewski, J. Alloys Compd. **509**, 578 (2011).
10. J.-L. Bobet, S. Pechev, B. Chevalier, and B. Darriet, J. Alloys Compd. **267**, 136 (1998).
11. E. Burzo, T. Crainic, M. Neumann, L. Chioncel, and C. Lazar, J. Magn. Magn. Mater. **290–291**, 371 (2005).
12. T. Toliński, G. Chelkowska, A. Hoser, and A. Kowalczyk, J. Alloys Compd. **442**, 286 (2007).
13. V. I. Anisimov, F. Aryasetiawan, and A. I. Lichtenstein, J. Phys.: Condens. Matter **9**, 767 (1997).
14. O. K. Andersen, Phys. Rev. B: Solid State **12**, 3060 (1975).
15. I. A. Nekrasov, E. E. Kokorina, V. A. Galkin, Yu. I. Kuz'min, Yu. V. Knyazev, and A. G. Kuchin, Physica B (Amsterdam) **407**, 3600 (2012).
16. Yu. V. Knyazev, A. V. Lukoyanov, Yu. I. Kuz'min, and A. G. Kuchin, Phys. Status Solidi B **249**, 824 (2012).
17. Yu. V. Knyazev, A. V. Lukoyanov, Yu. I. Kuz'min, and A. G. Kuchin, Phys. Solid State **55** (2), 385 (2013).
18. C. N. Berglund and W. E. Spicer, Phys. Rev. [Sect.] A **136**, 1044 (1964).
19. M. I. Kaganov and V. V. Slezov, Sov. Phys. JETP **5**, 1216 (1957).

Translated by G. Skrebtsov